Cancer Letters 450 (2019) 132–143

Contents lists available at ScienceDirect

Cancer Letters

journal homepage: www.elsevier.com/locate/canlet

Original Articles

PTK2 promotes cancer stem cell traits in hepatocellular carcinoma by activating Wnt/β-catenin signaling

Zhongyi Fan[a,1], Jingjing Duan[b,1], Lingxiong Wang[a,1], Saisong Xiao[c,1], Lingling Li[b], Xiang Yan[a], Wei Yao[a], Liangliang Wu[a], Sujie Zhang[a], Yong Zhang[a], Ye Li[a], Xiang Zhu[d], Yi Hu[a], Dong Zhang[e,***], Shunchang Jiao[a,**], Xiaojie Xu[d,*]

[a] Department of Oncology, The First Medical Centre, Chinese PLA General Hospital, Beijing, China
[b] School of Medicine, Nankai University, Tianjin, China
[c] Department of Anesthesia, Dongzhimen Hospital, Beijing University of Chinese Medicine, Beijing, China
[d] Department of Medical Molecular Biology, Beijing Institute of Biotechnology, Beijing, China
[e] Department of Oncology, The Second Medical Centre, Chinese PLA General Hospital, Beijing, China

ARTICLE INFO

Keywords:
FAK
HCC
CSCs
Sorafenib resistance
Methylation

ABSTRACT

Emerging evidence indicates that cancer stem cells (CSCs) are involved in tumorigenesis, tumor recurrence, and therapeutic resistance in hepatocellular carcinoma (HCC). However, the mechanisms underlying HCC CSC regulation remain largely unknown. Here we report our analysis of 97 paraffin-embedded HCC tumor specimens. We found that protein tyrosine kinase 2 (PTK2) expression correlated with liver CSC marker expression, overall survival, and recurrence-free survival in HCC patients. Our results further showed that PTK2 activated Wnt/β-catenin signaling by promoting nuclear accumulation of β-catenin in HCC cells. In this manner, PTK2 activates CSC traits and drives tumorigenicity in HCC cells, leading to HCC recurrence and sorafenib resistance. Moreover, PTK2 expression was negatively correlated with its level of promoter methylation. PTK2 apparently acts as an oncogene by increasing CSC traits and tumorigenicity in HCC. The present data suggest that PTK2 may be a novel prognostic biomarker for HCC recurrence, and a therapeutic target for HCC treatment.

1. Introduction

Liver cancer is a severe health problem, ranking as the fifth most prevalent malignancy and the third largest cause of cancer-related death worldwide [1,2]. The predominant histological subtype is hepatocellular carcinoma (HCC), which accounts for 70–85% of total liver cancer cases [3,4]. Despite therapeutic advances, HCC prognosis remains poor due to frequent recurrence after surgical resection, and poor responses to both conventional chemotherapy and the molecular targeted agent sorafenib [4–7]. Accumulating evidence indicates that HCC therapeutic resistance and recurrence are closely associated with liver cancer stem cells (CSCs) [8–10]. However, the detailed regulatory mechanisms controlling HCC CSCs remain largely unknown. Elucidation of these mechanisms is fundamental for the development of more effective therapeutic strategies to address HCC therapy resistance and recurrence.

The nonreceptor protein tyrosine kinase 2 (PTK2), also known as focal adhesion kinase (FAK), mediates the transduction of signals released from integrins and growth factor receptors [11–13]. Upon activation, PTK2 regulates diverse cellular functions, including cell adhesion, proliferation, migration, and survival [11,13–17]. Multiple studies demonstrate upregulated PTK2 expression and activity in many tumor types, which is associated with poor prognosis [14–16,18]. Several reports show PTK2 overexpression and hyperphosphorylation in HCC specimens [19–22], and recent studies describe a link between PTK2 and CSC regulation [23–25]. However, the role of PTK2 in HCC CSC regulation remains poorly understood [26–28], and the precise function and mechanisms of PTK2 in this context have not been established.

Abbreviations: CSCs, cancer stem cells; HCC, hepatocellular carcinoma; TCGA, The Cancer Genome Atlas; KEGG, Kyoto Encyclopedia of Genes and Genomes; GO, Gene ontology; GSEA, gene set enrichment analysis; PTK2, protein tyrosine kinase 2; FAK, focal adhesion kinase; OS, overall survival; HR, hazard ratio

* Corresponding author. Department of Oncology, The First Medical Centre, Chinese PLA General Hospital, 28 Fu-Xing Rd, Beijing, 100853, PR China.
** Corresponding author. Department of Medical Molecular Biology, Beijing Institute of Biotechnology, 27 Tai-Ping Rd, Beijing, 100853, PR China.
*** Corresponding author. Department of Oncology, The Second Medical Centre, Chinese PLA General Hospital, 28 Fu-Xing Rd, Beijing, 100853, PR China.
E-mail addresses: zhangdongjfjzyy@sina.com (D. Zhang), jiaosc301@163.com (S. Jiao), miraclexxj@126.com (X. Xu).
[1] These authors contributed equally to this work.

https://doi.org/10.1016/j.canlet.2019.02.040
Received 29 October 2018; Received in revised form 1 February 2019; Accepted 14 February 2019

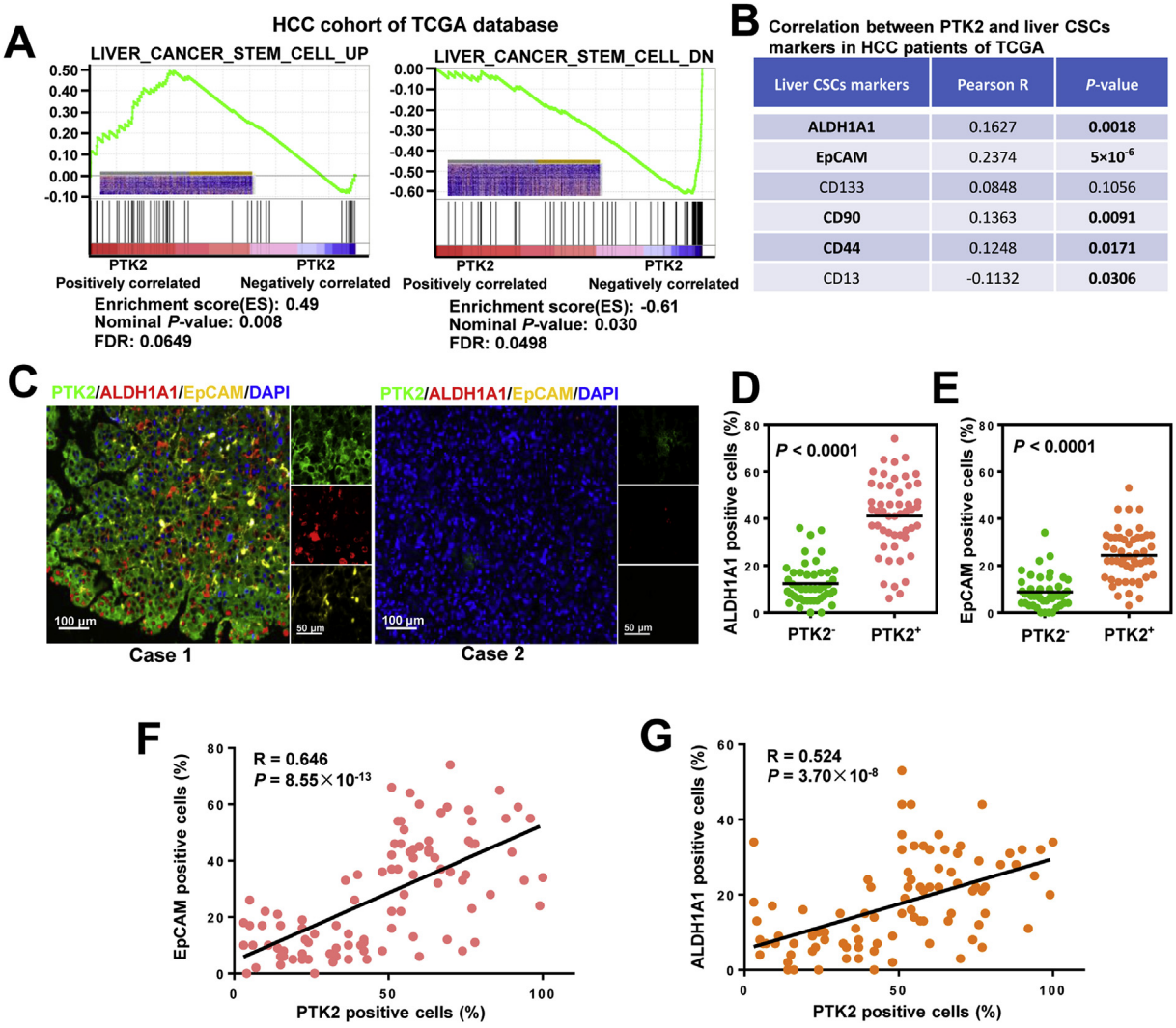

Fig. 1. PTK2 positively correlates with CSC marker expression in HCC. (A) GSEA plot showing that PTK2 expression is positively correlated with liver CSC-activated gene signatures, and inversely correlated with liver CSC-suppressed gene signatures in the TCGA HCC dataset. (B) Correlations between PTK2 expression and the major liver CSC markers ALDH1A1, EpCAM, CD90, and CD44. (C–E) Correlations of PTK2 protein expression with ALDH1A1 and EpCAM in tumor sections from 97 HCC specimens that were stained for immunofluorescence with anti-PTK2 and anti-ALDH1A1 or anti-EpCAM antibodies. (C) Representative images of immunofluorescence staining of PTK2, ALDH1A1, and EpCAM. Case 1 shows low PTK2 expression, and case 2 shows high PTK2 expression. (D and E) The percentage of ALDH1A1-positive (D) or EpCAM-positive (E) cells within the PTK2-positive and PTK2-negative cell populations. (F and G) Correlation analysis of the percentage of PTK2 positive cells with ALDH1A1 positive cells (F) or EpCAM positive cells (G) using Pearson correlation analysis. Data were compared using a two-tailed Student's *t*-test. Data are shown as mean ± SD. $^*P < 0.05$.

In the current study, we analyzed 97 paraffin-embedded HCC tumor specimens. Our results showed that PTK2 was overexpressed in HCC tissues and was positively correlated with the expression of liver CSC genes, recurrence, and poor patient survival. Our findings further suggested that PTK2 functionally stimulates the Wnt/β-catenin pathway by increasing CSC subpopulations in HCC. In this manner, PTK2 enhances tumorigenicity and sorafenib-resistance both *in vitro* and *in vivo*. We also demonstrated that PTK2 promoter hypomethylation is a novel molecular mechanism underlying PTK2 overexpression in HCC. Our present data suggest that PTK2 may be a novel prognostic biomarker for HCC recurrence, as well as a therapeutic target for HCC treatment.

2. Materials and methods

2.1. Clinical samples

This study included 97 archived paraffin-embedded HCC tumor specimens collected at the Chinese PLA General Hospital between 2014 and 2016. All tumors were histologically confirmed, and none of the patients had prior history of other cancers or previous chemotherapy or radiotherapy. All patients gave their informed consent, and this study was approved by the Institutional Review Committee of the Chinese PLA General Hospital.

2.2. Immunofluorescence analysis

In all tissue sections, immunofluorescence for PTK2, EpCAM, and ALDH1A1 expression was performed using OPAL-4-plex reagents (Perkin-Elmer, Shanghai, China) following the manufacturer's instructions. The utilized antibodies included rabbit anti-PTK2 (1:250, ab40794; Abcam, Cambridge, MA, USA), rabbit anti-ALDH1A1 (1:250, sc-374076; Santa Cruz, Dallas, TX, USA), and mouse anti-EpCAM (1:100, sc-25308; Santa Cruz). Standard immunofluorescence methods were used. Images were acquired with the Mantra Automated Quantitative Pathology Imaging System, and analyzed using Inform software (Perkin-Elmer).

Table 1
Univariate and multivariate analysis of various clinical parameters for RFS in patients with HCC by Cox-regression analysis from TCGA dataset.

Terms	Univariate analysis		Multivariate analysis	
	HR(95%CI)	P value	HR(95%CI)	P value
Age(years)				
< Median	1.00			
≥Median	0.970(0.719-1.308)	0.843	—	NA*
Gender				
Male	1.00			
Female	1.001(0.729-1.375)	0.995	—	NA*
Clinical Stage				
Stage I + II	1.00		1.00	
Stage III + IV	2.246(1.616-3.122)	**1 × 10-6**	1.812(0.445-7.386)	0.407
Tumor Size Classification				
T1 + T2	1.00		1.00	
T3 + T4	2.232(1.618-3.077)	**9.82 × 10-7**	1.247(0.302-5.152)	0.761
Lymphatic Metastasis				
No	1.00			
Yes	1.510(0.372-6.121)	0.564	—	NA*
Distant Metastasis				
No	1.00			
Yes	2.685(0.656-10.986)	0.169	—	NA*
Alcohol				
No	1.00			
Yes	1.070(0.748-1.531)	0.712	—	NA*
HBV				
No	1.00			
Yes	1.011(0.721-1.417)	0.951	—	NA*
HCV				
No	1.00			
Yes	1.120(0.747-1.679)	0.585	—	NA*
PTK2 Expression				
Low	1.00		1.00	
High	1.466(1.074-2.000)	**0.016**	1.431(1.035-1.977)	**0.030**

Bold P value indicates statistical significance.
* Not assessed due to an insignificant result in the univariate analysis (P > 0.1).

2.3. Cell culture and reagents

HepG2, MHCC-97H, Huh-7, SMMC-7721, BEL-7402, and LO2 cell lines were purchased from the American Type Culture Collection (ATCC). All cell lines were previously tested for mycoplasma contamination. Cells were routinely cultured in DMEM (Invitrogen, Carlsbad, CA, USA) or RPMI 1640 (Invitrogen) supplemented with 10% FBS (HyClone, Logan, UT, USA) and 1% penicillin/streptomycin (Invitrogen). Sorafenib (BAY 43-9006) was obtained from MedChemExpress (Shanghai, China). The Wnt inhibitor XAV939 (X3004) and the demethylation agent 5-aza-2′-deoxycytidine (5-AZA, A3656) were purchased from Sigma (St. Louis, MO, USA).

2.4. Lentiviruses and stable cell lines

Lentiviruses for PTK2 overexpression, and those carrying the PTK2 shRNA, were purchased from Genecreate (Wuhan, China). For stable cell line generation, HepG2 cells were infected with PTK2-overexpressing or PTK2-silencing lentivirus at a multiplicity of infection (MOI) of 10, followed by selection using 1 μg/ml puromycin for 2 months. Pooled clones were screened following standard immunoblot protocols.

2.5. Gene set enrichment analysis

Gene set enrichment analysis (GSEA) was performed using GSEA 2.2.3 software. PTK2 expression was treated as a numeric variable. We applied a continuous-type cls file of the PTK2 profile to phenotype labels. The metric for ranking genes in GSEA was set as 'Pearson', and the other parameters were set to default values.

2.6. Western blot analysis

Western blotting was performed following standard methods. The utilized antibodies included anti-PTK2 (1:500, ab40794; Abcam), anti-phospho-PTK2 (Tyr397) (1:500, 44-624G; Invitrogen), anti-β-catenin (1:500, ab16051; Abcam), anti-Lamin A/C (1:1,000, sc-20681; Santa Cruz), and anti-Tubulin (1:1,000, 11224-1-AP; Proteintech, Chicago, IL, USA). Anti-GAPDH (1:2,000, SAB2108266; Sigma) was used as a loading control.

2.7. RNA extraction and RT-PCR

Total mRNA was extracted using the RNA Extraction Kit (Takara Bio Inc., Shiga, Japan) following the manufacturer's protocol. RNA was reverse transcribed into cDNA using the PrimeScript™ RT Reagent Kit (Takara Bio Inc.). Then real-time PCR was performed using SYBR Premix Ex Taq™ (Takara Bio Inc.) and the primers listed in Supplementary Table 4.

2.8. Subcellular fractionation

Cells were homogenized using a Dounce homogenizer, and the homogenate was centrifuged at 366 × *g* for 10 min. The pellet was analyzed as the nuclear fraction, while the supernatant was centrifuged at 16,200 × *g* for 10 min. The final supernatant was analyzed as the cytoplasmic fraction.

2.9. Sphere formation assay

We seeded 1,000 cells in 6-well ultra-low adhesion plates (Corning Inc., Tewksbury, MA, USA), and incubated them for 10 days. The generated spheres were cultured in DMEM/F12 serum-free medium (Invitrogen) supplemented with 2% B27 (BD Biosciences, San Jose, CA, USA), 20 ng/ml EGF, 20 ng/ml bFGF, 0.4% BSA, and 5 mg/ml insulin (Sigma).

2.10. Limiting dilution assay

Cells were dissociated into single cells, and then seeded in 96-well plates at a density of 1, 5, 10, or 25 cells per well. After 7 days, each well was examined for tumorsphere formation. Extreme limiting dilution assays were analyzed using software available at http://bioinf.wehi.edu.au/software/elda.

2.11. Flow cytometric analysis

We assessed the aldehyde dehydrogenase 1 (ALDH1) enzyme activity in viable cells using Aldefluor® assays (Stem Cell Technologies, Vancouver, BC, Canada) following the manufacturer's instructions. To confirm specificity, diethylaminobenzaldehyde (DEAB) was used to inhibit ALDH activity. We analyzed EpCAM + cells using a PE-conjugated anti-EpCAM antibody (Biolegend, San Diego, CA, USA) following the manufacturer's instructions. Briefly, cultured cells (5×10^5 cells) were centrifuged. The cell pellets were resuspended in blocking buffer, and then incubated with antibody. Cells were then washed in blocking buffer, and fluorescent staining was visualized by flow cytometry (FACSCalibur; Becton Dickinson, Franklin Lakes, NJ, USA). Data were analyzed using a FACSCalibur Flow Cytometer (Becton

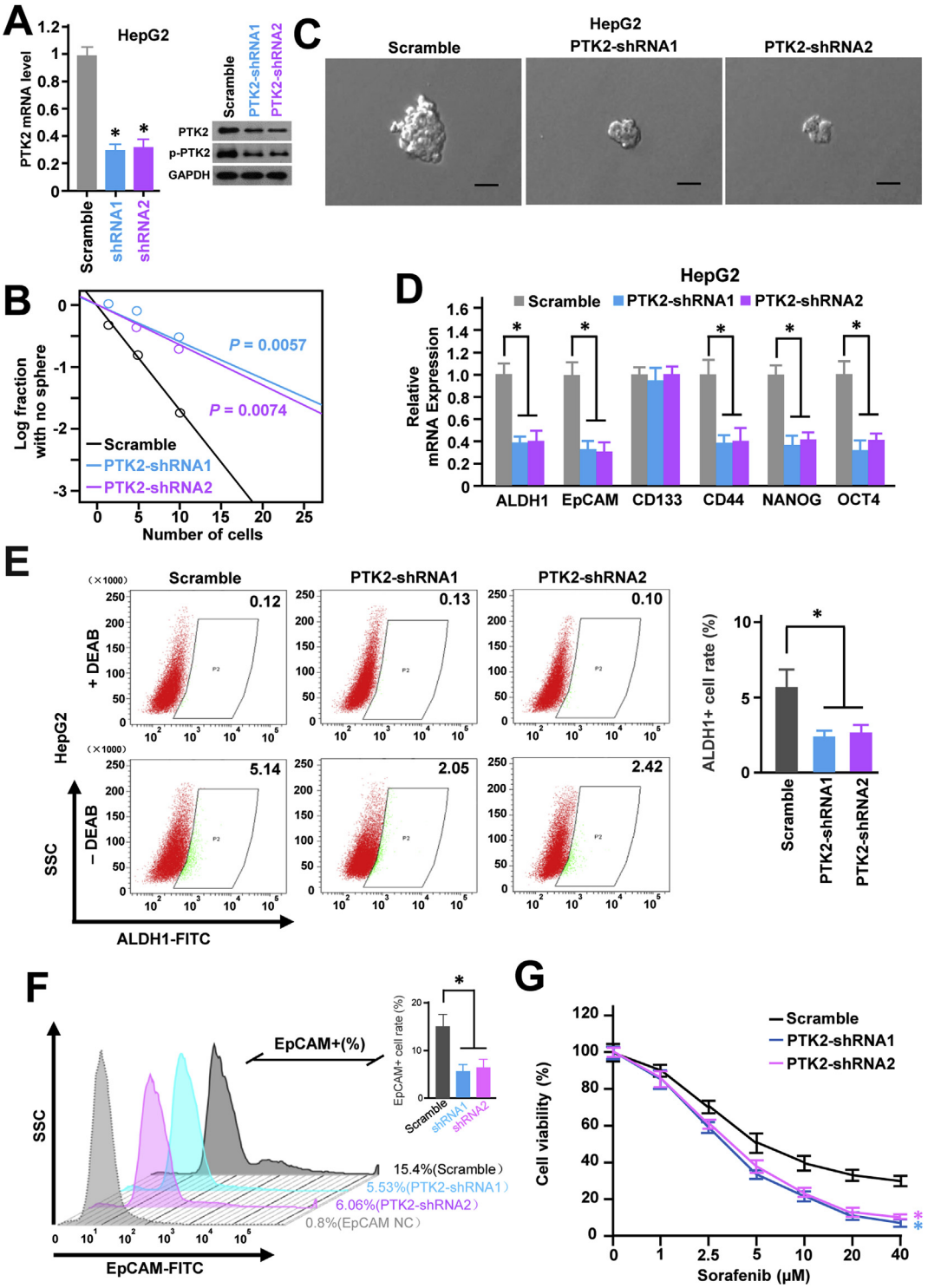

Fig. 2. PTK2 promotes a CSC-like phenotype in HCC cells. (A) RT-PCR for PTK2 mRNA (left), and immunoblotting for total PTK2 and p-PTK2 (Tyr397) protein expression (right) in stable PTK2-knockdown HepG2 cells. (B) *In vitro* limiting dilution assays showing the tumorsphere formation frequency in control and PTK2-silenced cells. (C) Representative images of spheres formed by the indicated cells. Scale bar: 50 μm. (D) RT-PCR analysis of the mRNA expression levels of the HCC CSC-associated markers ALDH1, EpCAM, CD133, CD44, NANOG, and OCT4 in PTK2-silenced and control cells. (E) Analysis of ALDH-high cell percentages by Aldefluor assays in the indicated cells. To show specificity, diethylaminobenzaldehyde (DEAB) was used to inhibit ALDH activity. (F) Flow cytometry analysis of the EpCAM + cell distribution in the indicated cells. HepG2 cells without EpCAM-FITC served as the EpCAM negative control. (G) Cell viability assays in PTK2 knockdown and control cells treated with the indicated sorafenib concentrations for 72 h. Untreated cells were set as 100% viability. Data are shown as the mean ± SD from three independent experiments. *$P < 0.05$.

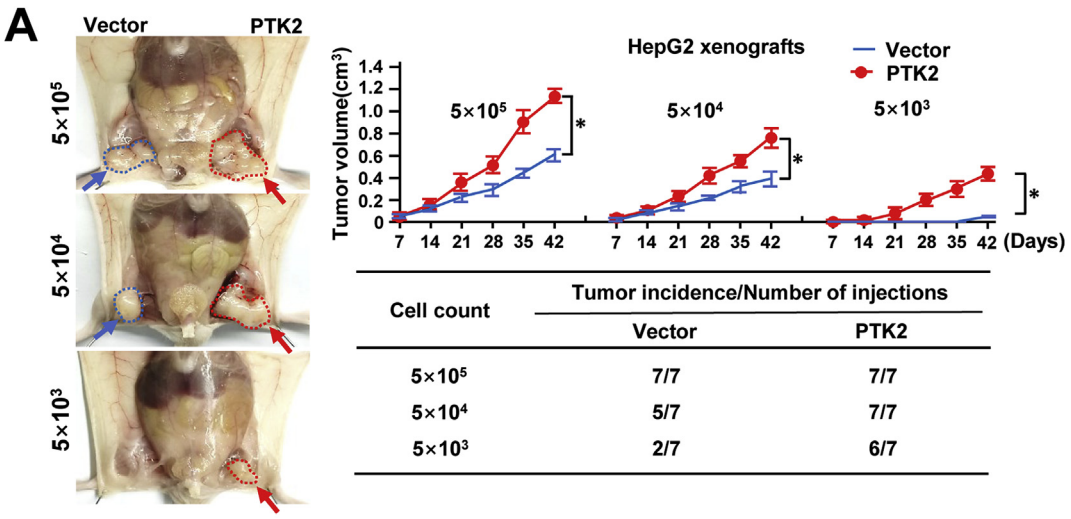

Cell count	Tumor incidence/Number of injections	
	Vector	PTK2
5×10^5	7/7	7/7
5×10^4	5/7	7/7
5×10^3	2/7	6/7

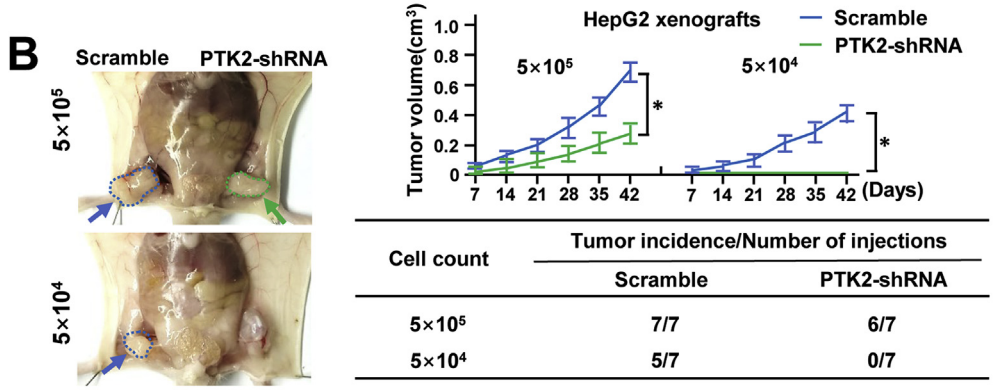

Cell count	Tumor incidence/Number of injections	
	Scramble	PTK2-shRNA
5×10^5	7/7	6/7
5×10^4	5/7	0/7

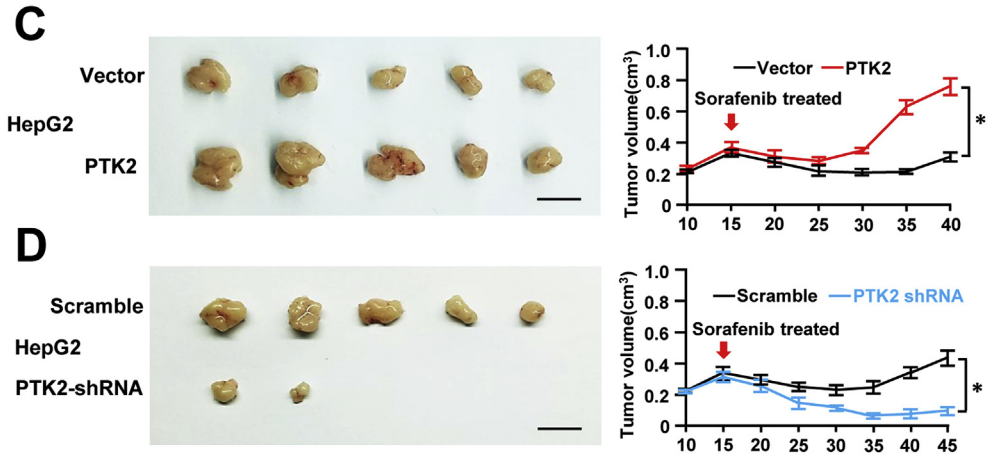

Fig. 3. PTK2 enhances HCC tumorigenicity and tumor recurrence. (A and B) Tumor xenografts were generated using the indicated numbers of PTK2-overexpressing (A) or PTK2-knockdown (B) HepG2 cells, and compared with the corresponding control cells. Representative images of the tumors are shown on the left. On the right, tumor growth curves (upper panel) and tumor formation frequencies (lower panel) are shown for each group. Data are shown as mean ± SD. *$P < 0.05$. (C and D) Nude mice were subcutaneously injected with PTK2-overexpressing or PTK2-knockdown HepG2 cells (1×10^7). When the mean tumor volume reached 0.3 cm^3 (day 15), the mice were treated orally with sorafenib (30 mg/kg) daily for 1 week. Representative images of the tumors are shown on the left. Tumor growth curves are shown on the right. Scale bar, 1 cm. Data are shown as mean ± SD. *$P < 0.05$ (two-tailed Student's *t*-test).

Dickinson).

2.12. In vivo tumor xenografts

Animal studies were performed in accordance with protocols approved by the Institutional Animal Care and Use Committee at Chinese PLA General Hospital. Male 6-week-old BALB/c nu/nu mice were randomly divided into five groups (n = 7 per group), and subcutaneously injected in the left inguinal folds with PTK2-overexpressing HepG2 cells (5×10^5, 5×10^4, or 5×10^3 cells) or PTK2-silenced HepG2 cells (5×10^4 or 5×10^3 cells). The mice were injected on the right side with the corresponding control cells. Tumor growth was monitored, and tumor size was measured using calipers. At 42 days after inoculation, mice were anesthetized and euthanized.

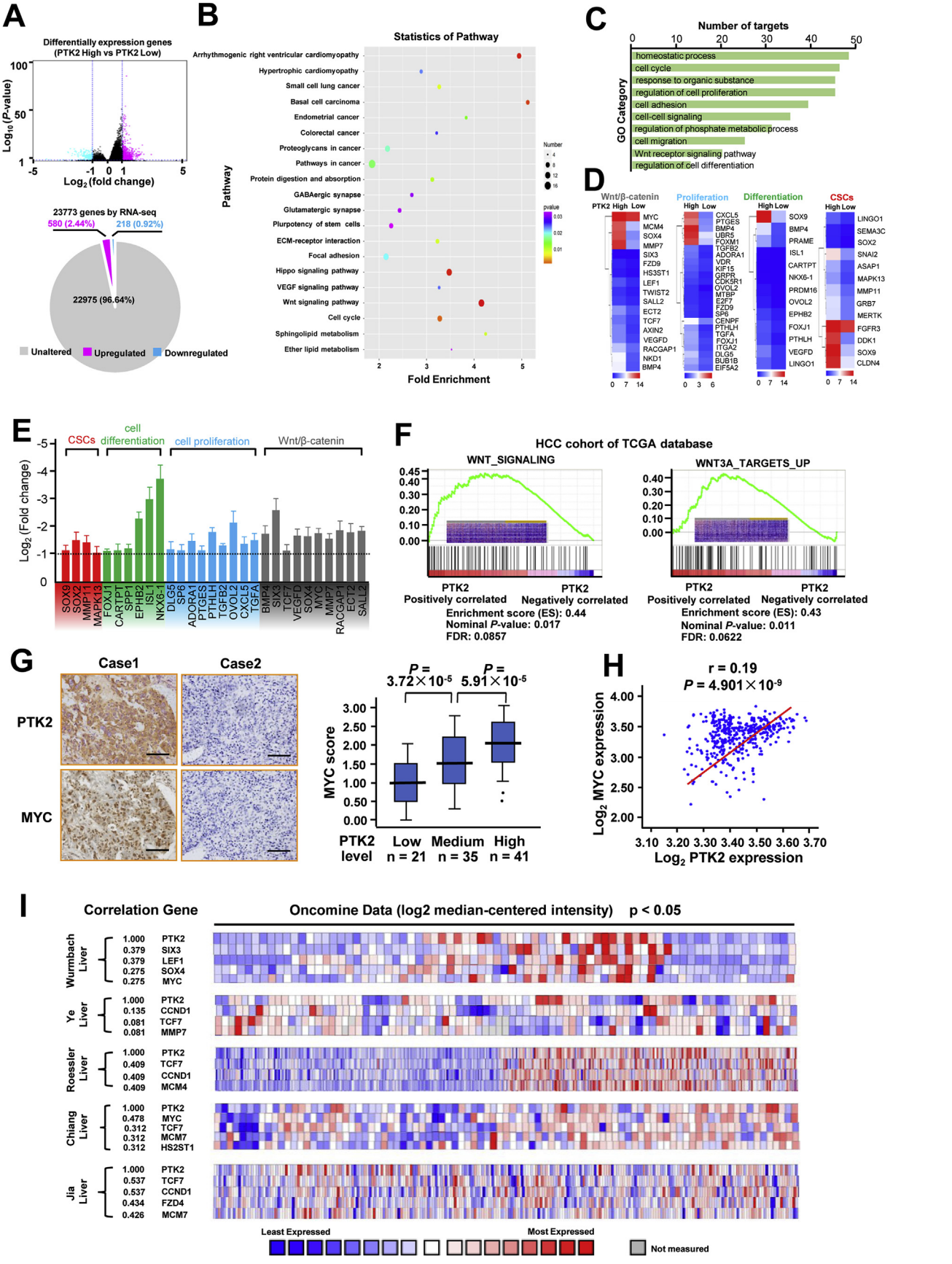

(caption on next page)

Fig. 4. Characterization of gene expression changes between PTK2-high and PTK2-low expression groups in the TCGA HCC dataset. (A) Volcano plot illustrating genes that are differentially expressed between the PTK2-high and PTK2-low expression groups in the TCGA HCC RNA-seq dataset. Upregulated genes are shown in purple, and downregulated genes in blue. (B) KEGG pathway analysis of upregulated targets in the PTK2-high expression group. (C) The top 10 most significantly affected pathways revealed by gene ontology (GO) analysis of PTK2 upregulated genes. (D) Heat-maps showing representative genes in the Wnt/β-catenin, cell proliferation, cell differentiation, and CSC pathways in the PTK2-high and PTK2-low groups. (E) Results of qRT-PCR confirming downregulation of genes in the indicated signaling pathways in PTK2-silenced cells. (F) GSEA plot showing PTK2 expression in association with Wnt signaling-related genes. (G) On the left, representative IHC images from 97 liver cancer patient samples assessed by IHC for PTK2 and MYC. Case 1 shows low PTK2 expression, and case 2 shows high PTK2 expression. Scale bar, 100 μm. The right panel shows the correlation between PTK2 and MYC, analyzed by one-way ANOVA with Games-Howell correction. Horizontal lines inside the box represent the median. The bottom and top of the box represent the 25th and 75th percentile, respectively. The lines above and below the box represent the upper and lower extremes. The vertical bars represent the data range. Outliers are marked with a circle. (H) Analysis of the correlation between PTK2 and MYC mRNA expression using data from The Genome Cancer Atlas (TCGA), with the following filters: Disease type, liver cancer; Data category, transcriptome profiling; Data type, gene expression quantification; Experimental strategy, RNA-Seq; Workflow type, HTSeq–FPKM; and Access level, open. (I) Analysis of the correlation between PTK2 and Wnt target gene mRNA expression levels using the data from Oncomine, with the following filters: Gene, PTK2; Analysis type, coexpression analysis; and Data type, mRNA. Colors indicate weaker (blue) or higher (red) expression, passing by white, with fluctuating color intensity. (For interpretation of the references to color in this figure legend, the reader is referred to the Web version of this article.)

To analyze tumor relapse, mice (n = 5 per group) were inoculated with 1×10^7 PTK2-overexpressing or PTK-silenced HepG2 cells. When the mean tumor volume reached approximately 0.3 cm^3 (~15 days), the mice were orally treated with sorafenib (30 mg/kg) every day for one week. On day 45 after injection, the animals were euthanized, anatomized, and photographed. Tumor volumes were estimated using equation $(L \times W^2)/2$.

2.13. DNA extraction and DNA methylation analysis

Genomic DNA was extracted from HCC cell lines and HCC tumor tissues using the Universal Genomic DNA Extraction Kit (TaKaRa) following the manufacturer's instructions. We quantified the DNA methylation of CpG dinucleotides using the Sequenom MassARRAY EpiTYPER (Sequenom Inc., San Diego, CA, USA).

2.14. Statistical analysis

We assessed sample sizes for adequate statistical power based on trial experiments and previously performed similar experiments. Survival curves were analyzed using the Kaplan-Meier method, and significance was assessed by log-rank test. Univariate and multivariate analyses were performed using Cox regression analysis. We evaluated the correlation between methylation levels and PTK2 expression using Spearman's rank correlation test. Between-group comparisons were assessed using a two-tailed Student's *t*-test. All statistical tests were two-sided. Statistical calculations were performed using SPSS 13.0. Data are presented as mean ± standard deviation (SD). In all assays, $P < 0.05$ was considered statistically significant.

3. Results

3.1. PTK2 correlates with CSC marker expression and is a negative prognostic factor for HCC

To examine the role of PTK2 in HCC, we performed gene set enrichment analysis (GSEA). We searched for functional signaling pathways that were closely correlated with PTK2 expression, stratified according to the best cutoff based on receiver operating characteristic curve analysis. Interestingly, a defined set of liver CSC genes exhibited a positive correlation with PTK2 expression levels in The Cancer Genome Atlas (TCGA) HCC dataset (Fig. 1A). This suggested that PTK2 promotes increased CSC traits in HCC. Moreover, the expressions of many major liver CSC markers (including ALDH1A1, EpCAM, CD90, and CD44) were positively correlated with PTK2 expression (Fig. 1B). Immunofluorescence analysis revealed the positive percentage of CSC markers is higher in PTK2 positive group than in the PTK2 negative group (Fig. 1C–E), suggesting that PTK2 is associated with CSCs in HCC. To further confirm the relation of PTK2 and CSC markers, we evaluated the positive cell rates of PTK2 and CSC markers in each HCC samples and performed statistical correlation assay (Fig. 1F and G). Our result showed that PTK2 expression was positively correlated with CSC markers, such as ALDH1A1 ($R = 0.646$, $P = 8.55 \times 10^{-13}$) and EpCAM ($R = 0.524$, $P = 3.70 \times 10^{-8}$).

To examine PTK2 expression in HCC patients, we used the cBioPortal program (http://www.cbioportal.org/) to screen for PTK2 status among cases of HCC in the TCGA database. Among 440 HCC cases, 174 (40%) had altered PTK2 expression, of which 166 (38%) showed PTK2 overexpression due to either gene amplification or mRNA upregulation (Supplementary Fig. 1A). We next evaluated PTK2 expression in 50 paired HCC samples from the TCGA dataset, which revealed marked PTK2 overexpression in tumor tissues compared to nontumor tissues (Supplementary Fig. 1B). Moreover, PTK2 was universally expressed at higher levels in five HCC cell lines compared to in normal human hepatocyte LO2 cells (Supplementary Fig. 1C and D). Further analysis of the TCGA HCC dataset uncovered that patients with higher PTK2 expression exhibited a significantly higher recurrence rate ($P = 0.0153$) and shorter overall survival (OS) ($P = 0.0302$) compared to patients expressing lower PTK2 levels (Supplementary Fig. 1E and 1F). Univariate analysis also showed a significant association between increased PTK2 expression and increased mortality among HCC cases in the TCGA dataset ($P = 0.016$).

Next, we performed Cox regression multivariate analysis including factors for which P was ≤ 0.1 in the univariate analysis. The multivariate analysis was adjusted for patient age at diagnosis, pathologic type, TNM stage, alcohol consumption, and HBV and HCV infection status. The results demonstrated that PTK2 expression was significantly associated with shorter recurrence-free survival among patients with HCC, with a hazard ratio (HR) of 1.431 (95% CI, 1.035–1.977; $P = 0.030$) (Table 1). Similar results were obtained for OS in HCC patients (Supplementary Table 1). We also found significantly higher PTK2 expression in grade 1 HCC than in HCC of other grades; however, PTK2 level did not significantly differ between tumors of grades 2–4 (Supplementary Fig. 2A). PTK2 expression was not correlated with HBV or HCV infection (Supplementary Fig. 2B), suggesting that PTK2 overexpression is a general feature of HCC and is not associated with common etiological factors. Our data supported that PTK2 overexpression was frequent in HCC, and may predict adverse prognosis in HCC patients.

3.2. PTK2 promotes a stem cell-like phenotype in HCC

To investigate the functional role of PTK2 in HCC, we induced the stable overexpression or knockdown of PTK2 (sh-PTK2) in HepG2 cells, which have median endogenous PTK2 expression levels. We also confirmed PTK2 silencing in MHCC97H cells. The sh-PTK2 and PTK2-overexpressed HepG2 cell lines were analyzed by RT-PCR and western blotting to confirm successful knockdown and overexpression of PTK2 mRNA, total protein, and phosphoprotein levels (Fig. 2A and Supplementary Fig. 3A). PTK2 knockdown significantly decreased

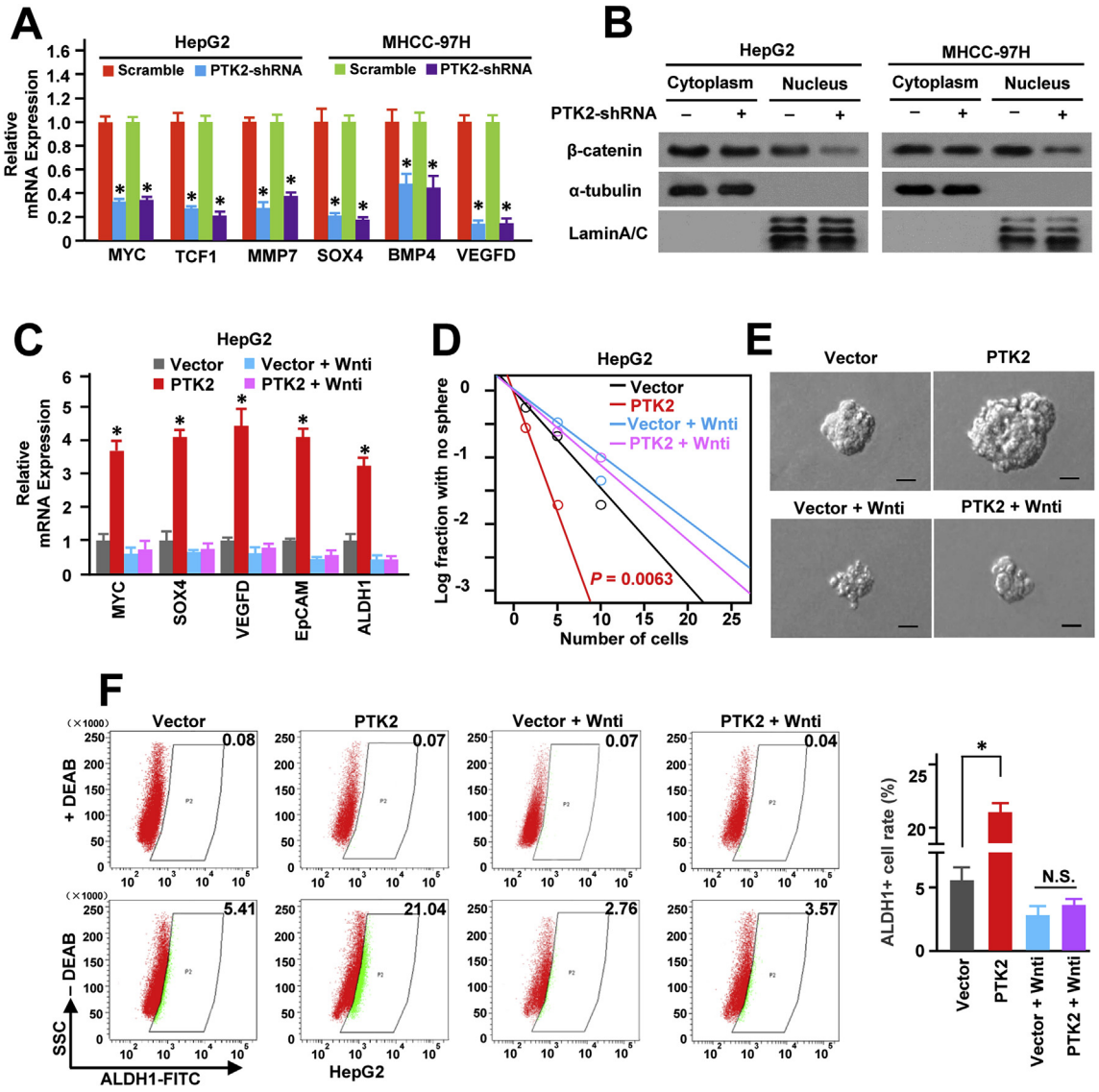

Cell count	Tumor incidence/Number of injections			
	Vector	PTK2	Vector + Wnti	PTK2 + Wnti
5×10^5	7/7	7/7	6/7	7/7
5×10^4	5/7	7/7	1/7	1/7
5×10^3	2/7	5/7	0/7	0/7

(caption on next page)

Fig. 5. PTK2 activation of Wnt/β-catenin signaling contributes to CSC maintenance and HCC tumorigenicity. (A) RT-PCR analysis of mRNA expression levels of the Wnt/β-catenin pathway targets MYC, TCF7, MMP7, SOX4, BMP4, and VEGFD in the indicated cells. (B) Subcellular localization of β-catenin determined by analyzing the cytoplasmic and nuclear fractions of the indicated cells, with α-tubulin and LaminA/C used as cytoplasmic and nuclear fraction controls, respectively. (C) RT-PCR analysis of mRNA expression levels of MYC, SOX4, VEGFD, EpCAM, and ALDH1 in PTK-overexpressing or control cells treated with WNT inhibitor (5 μM) for 72 h. (D) *In vitro* limiting dilution assays showing the frequency of tumorsphere formation in PTK-overexpressing or control cells treated with WNT inhibitor (5 μM) for 72 h. (E) Representative images of spheres formed by the indicated cells. Scale bar: 50 μm. (F) ALDH-high cell percentages analyzed by Aldefluor assays in the indicated cells. DEAB was used to inhibit ALDH activity. (G) Tumor formation frequencies in mice treated with either vehicle (DMSO, Sigma) or XAV939 at 50 mg/kg/d i.p. daily. Data are shown as the mean ± SD from three independent experiments. For A, C, and F, a two-tailed Student's *t*-test was used for statistical analysis. $^{*}P < 0.05$.

tumorsphere formation rates in *in vitro* limiting dilution assays (Fig. 2B), which are a widely used method of evaluating the self-renewal capacity of CSCs. The PTK2-silenced HepG2 cells also formed smaller spheres than control cells (Fig. 2C). On the other hand, PTK2-overexpressing cells formed greater numbers of tumorspheres and larger spheres compared to control cells (Supplementary Fig. 3B and C). Notably, the mRNA expression levels of liver CSC markers (including ALDH1, EpCAM, CD44, NANOG, and OCT4, but not CD133) were significantly reduced in PTK2-silenced cells and increased in PTK2-overexpressing cells (Fig. 2D and Supplementary Fig. 3D). Additionally, the proportions of $ALDH1^+$ and $EpCAM^+$ cells were decreased in PTK2-silenced cells and upregulated in PTK2-overexpressing cells (Fig. 2E and F, and Supplementary Fig. 3E and F). Similar results were obtained in MHCC97H cells with PTK2 knockdown (Supplementary Fig. 4A–E).

Since CSCs are involved in HCC cells' resistance to sorafenib [8,26], we also examined how PTK2 affected the response of HepG2 cells to sorafenib. PTK2-silenced HepG2 cells showed a markedly increased response to sorafenib, while PTK2-overexpressing HepG2 cells exhibited a decreased sorafenib response (Fig. 2G and Supplementary Fig. 3G). These data supported the notion that PTK2 strongly enhanced the stem-like characteristics of HCC cells, promoting HCC recurrence and sorafenib resistance *in vitro*.

3.3. PTK2 enhances HCC tumorigenicity and tumor recurrence

We next examined the effects of PTK2 overexpression and knockdown on HCC tumorigenicity and recurrence *in vivo*. BALB/c nude mice were subcutaneously injected with different doses of PTK2-overexpressing HepG2 cells, PTK2-silenced HepG2 cells, or the corresponding control cells. Compared to the corresponding control cells, PTK2-overexpressing cells displayed higher tumorigenicity and increased tumor growth rates (Fig. 3A), while PTK2-silenced cells showed decreased tumorigenicity and slower growth rates (Fig. 3B). Similar results were obtained in MHCC-97H cells with PTK2 knockdown (Supplementary Fig. 4F).

To determine whether PTK2 was associated with HCC relapse, we next examined tumor growth in response to sorafenib treatment. Mice were injected with PTK2-overexpressing or PTK-silenced HepG2 cells. After the mean tumor volume reached approximately 0.3 cm^3 (approximately 15 days), mice were treated with sorafenib daily for 1 week. Tumors from PTK2-overexpressing cells and control cells both showed an initial transient reduction in tumor volume. Starting at day 25, tumors formed by PTK2-overexpressing cells showed increased growth compared to tumors from control cells (Fig. 3C). In contrast, tumors formed from PTK2-silenced cells exhibited a continual decrease of tumor growth until the experimental endpoint (day 45), whereas tumors formed by scramble-transduced cells showed slow and gradual regrowth (Fig. 3D). Compared to recurrent tumors from the corresponding control cells, recurrent tumors from PTK2-overexpressing cells were larger, while the recurrent tumors from PTK2-silenced cells were smaller. These data support the hypothesis that PTK2 strongly enhanced HCC cell tumorigenesis and contributed to HCC recurrence *in vivo*.

3.4. Analysis of downstream targets of PTK2 in HCC

To examine the potential targets of PTK2 that could be involved in mediating CSC traits and tumorigenicity in HCC, we performed RNA-seq data analysis in cases of high and low PTK2 expression in the TCGA HCC dataset. A total of 798 genes showed significantly differential expression (fold change > 2, $P < 0.05$ and adj $P < 0.05$) between cases with high versus low PTK2 expression (Supplementary Table 2). Of these, 580 (2.44%) were upregulated and 218 (0.92%) were downregulated in the PTK2-high expression group compared to the PTK2-low expression group (Fig. 4A). Kyoto Encyclopedia of Genes and Genomes (KEGG) pathway analysis revealed that the differentially expressed genes were enriched in genes involved in focal adhesion, ECM-receptor interactions, and Wnt signaling (Fig. 4B)—processes which are crucial for CSC activity and are involved in HCC recurrence [27]. Gene ontology (GO) analysis demonstrated that the differentially expressed genes showed significant enrichment of gene sets involved in regulating cell proliferation, regulating cell differentiation, cell adhesion, and the Wnt receptor signaling pathway (Fig. 4C). The main genes in these pathways were downregulated by over 2-fold in the PTK2-low expression group compared to the PTK2-high expression group (Fig. 4D). These findings were validated by qRT-PCR (Fig. 4E).

Since multiple analyses indicate an association of PTK2 with the Wnt signaling pathway, we further performed GSEA analysis to investigate this potential link. PTK2 expression was positively correlated with both the Wnt and Wnt3A signaling pathways (Fig. 4F). Analysis of samples from liver cancer patients demonstrated that PTK2 expression was positively correlated with the expression of MYC, a critical target gene of Wnt signaling (Fig. 4G). We additionally validated the correlations of PTK2 with MYC and with Wnt signaling targets by using external datasets from TCGA and Oncomine, respectively (Fig. 4H and I).

3.5. PTK2 activates Wnt signaling to promote CSC traits

Based on the results of RNA-seq analysis, we next examined the potential mechanism underlying the role of PTK2-mediated Wnt signaling in HCC CSC regulation. PTK2 knockdown significantly suppressed the expressions of well-established downstream target genes of the Wnt/β-catenin pathway. Conversely, PTK2 overexpression increased Wnt/β-catenin pathway activity (Fig. 5A and Supplementary Fig. 5A). Subcellular fractionation and immunoblot assays revealed that PTK2 silencing blocked the nuclear accumulation of β-catenin, while the opposite results were observed in response to PTK2 overexpression. This suggested that PTK2 activated Wnt/β-catenin signaling by reducing β-catenin degradation and increasing its nuclear accumulation in HCC cells (Fig. 5B and Supplementary Fig. 5B).

To verify whether PTK2 regulated Wnt/β-catenin target genes through the Wnt/β-catenin pathway, we treated cells with a Wnt signaling inhibitor. This inhibitor blocked the ability of PTK2 to induce Wnt/β-catenin target gene expression (Fig. 5C). Importantly, Wnt signaling inhibition also made PTK2-overexpressing cells unable to form spheres, enhance $ALDH1^+$ cells *in vitro*, and promote tumor growth *in vivo* (Fig. 5D–G). These data suggested that PTK2 promoted CSC-like characteristics and tumorigenicity by enhancing Wnt/β-catenin activity in HCC cells.

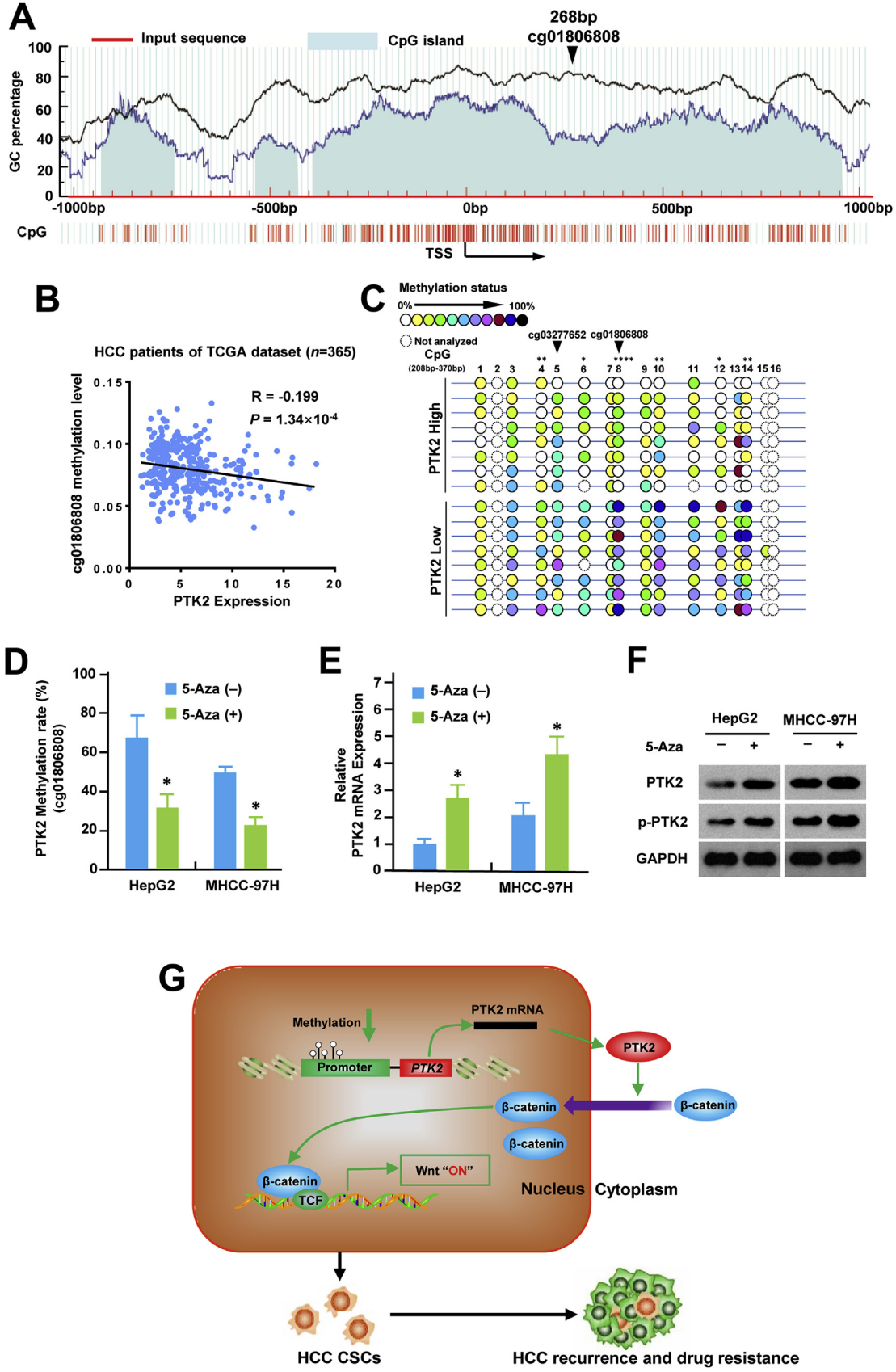

(caption on next page)

Fig. 6. Promoter hypomethylation drives PTK2 upregulation in HCC. (A) Schematic of the CpG islands in the *PTK2* promoter. Input sequence: red region; CpG islands: blue region; TSS: transcription start site; cg01806808: the CG sites in the *PTK2* CpG islands, identified using the TCGA dataset. (B) The relationship between cg01806808 methylation levels and PTK2 expression was assessed using Spearman's rank correlation analysis. Symbols represent individual samples. (C) MassARRAY-based quantitative analysis of DNA methylation levels in the *PTK2* promoter region containing the cg01806808 site in both PTK2-high and PTK2-low expression cases. (D) Methylation levels of the cg01806808 site were detected by MassARRAY in HepG2 and MHCC-97H cells treated with the demethylation agent 5-aza-2′-deoxycytidine (5-AZA, 5 μM) for 72 h. (E and F) RT-PCR analysis of PTK2 mRNA (E) and immunoblot analysis of PTK2 protein (F) in the indicated cell lines following treatment with 5-AZA (5 μM) for 72 h. For C and D, all values are shown as the mean ± SD from three independent experiments. $^{*}P < 0.05$. (G) The proposed model for the role of the PTK2/Wnt/β-catenin axis in regulating HCC CSC traits and tumorigenicity. PTK2 promoter hypomethylation induces PTK2 overexpression in HCC. PTK2 enhances stem cell-like traits by activating Wnt signaling, leading to HCC tumorigenicity and contributing to recurrence and sorafenib resistance. (For interpretation of the references to color in this figure legend, the reader is referred to the Web version of this article.)

3.6. PTK2 upregulation in HCC is due to promoter hypomethylation

Our findings showed that PTK2 was markedly overexpressed in HCC tumor tissues compared to in nontumor tissues. To investigate the mechanism underlying PTK2 overexpression in HCC, we examined aberrantly methylated promoter regions of the *PTK2* gene. We identified 20 CpG sites in these regions (Supplementary Table 3), of which 15 sites had a P value of ≤ 0.1 in univariate analysis. Linear regression multivariate analysis revealed that five CpG sites (cg01581024, cg01806808, cg10996527, cg14396066, and cg23913941) were negative regulators of PTK2 expression (Supplementary Table 3). Notably, cg01806808 was located in the CpG islands of the *PTK2* promoter region (Fig. 6A) and its methylation level was negatively associated with PTK2 expression ($r = -0.199$, $P = 1.34 \times 10^{-4}$) (Fig. 6B). At the four other CpG sites, methylation levels were also inversely correlated with PTK2 expression, but these sites were not located in CpG islands (Supplementary Fig. 6). MassARRAY-based quantitative DNA methylation analysis revealed that the total methylation level of the *PTK2* promoter CpG islands between 208 and 370 bp was significantly decreased in PTK2-high expression cases compared to PTK2-low expression cases, especially at the cg01806808 site (Fig. 6C). Moreover, HCC cells treated with the demethylation agent 5-AZA showed reduced *PTK2* (cg01806808) methylation levels, increased PTK2 mRNA levels, and increased total PTK2 and phospho-PTK2 protein levels (Fig. 6D–F). Overall, these results suggested that *PTK2* promoter methylation levels regulated PTK expression levels in HCC.

4. Discussion

HCC treatment is significantly limited by frequent recurrence and therapeutic resistance, both of which have been linked to liver CSCs. Thus, elucidation of the molecular mechanisms underlying CSC regulation could be of great clinical benefit in HCC. PTK2 is implicated as a positive regulator of the pathogenesis and progression of various cancers, including HCC [14–19]. Our present results demonstrated that PTK2 expression is likely an important contributor to HCC recurrence and sorafenib resistance. We further found that *PTK2* promoter hypomethylation induced PTK2 overexpression in HCC, and that PTK2 enhanced CSC-like traits by activating Wnt signaling, contributing to HCC cell tumorigenicity, recurrence, and sorafenib resistance (Fig. 6G). In addition, PTK2 was identified as a novel independent risk factor for HCC, with PTK2 overexpression predicting poor prognosis in HCC patients. Overall, these data suggest that PTK2-targetting inhibitors may control HCC recurrence and promote the reversal of sorafenib resistance. Indeed, several PTK2 inhibitors (i.e., GSK2256098, VS-6063, and defactinib) have been tested in phase I and II clinical trials for advanced tumors (https://clinicaltrials.gov/) [28–30]. Our current findings support the continued study of PTK2 inhibitors for HCC.

CSCs are a rare population of cancer cells with indefinite self-renewal potential, and which contribute to tumorigenesis, tumor recurrence, metastasis, and therapeutic resistance [31]. Therefore, targeting CSCs is a promising therapeutic strategy for addressing tumor recurrence and metastasis following chemotherapeutic resistance development. Several studies in HCC confirm that liver CSCs play an important role in maintaining hepatic tumorigenic properties [6,8,9,32]. Here we demonstrated that PTK2 promoted *in vitro* sphere formation and *in vivo* tumorigenicity, which are both important CSC characteristics, suggesting that PTK2-overexpressing HCC cells exhibit CSC traits. Moreover, PTK2-overexpressing HCC cells exhibited a propensity for recurrence and sorafenib resistance. We also found that PTK2 simultaneously increased the ratios of ALDH+ and EpCAM + cells, supporting that PTK2 plays an important role in maintaining CSC traits in HCC.

Aberrant Wnt signaling activation is frequently associated with CSC activation, and is essential for maintaining the stem cell phenotype. Thus, targeting Wnt signaling activity in CSCs may represent an important cancer therapy approach. Aberrant Wnt pathway activity is commonly associated with mutation of the β-catenin gene, and the frequency of somatic β-catenin gene mutations in HCC ranges between 20% and 40% [27,33]. Moreover, cytoplasmic and nuclear accumulation of β-catenin has been detected in 40–70% of HCC cases [27,34]. Thus, understanding the molecular mechanisms underlying mutations in Wnt pathway components, as well as hyperactivation of Wnt signaling, will be highly valuable for the development of novel therapeutic strategies aimed at HCC CSCs. Our present data revealed that PTK2 overexpression activated Wnt/β-catenin signaling by reducing β-catenin degradation and increasing the nuclear accumulation of β-catenin in HCC cells, consistent with observations in other cancers [21,35]. These findings advance our present understanding of how the PTK2-mediated stem-cell-like properties of HCC cells develop, and suggest that Wnt/β-catenin inhibitors may be a useful therapeutic agent to treat HCC patients presenting with PTK2 overactivation, recurrence, and sorafenib resistance.

While the B-RAF and EGFR tyrosine kinases are frequently mutated in cancer, *PTK2*-activating mutations were found in only 2% (10 of 440 cases) of HCC patients (Supplementary Fig. 1A) (http://www.cbioportal.org). Clarifying the mechanism of PTK2 overactivation is critical for the future development of related therapeutic strategies. Several studies demonstrate that PTK2 overexpression in HCC is mainly due to gene amplification [36–39]. However, two studies report low frequencies of *PTK2* gene amplification in HCC cases, ranging from 1.3% to 15.6% [36,37]. Therefore, other mechanisms must be responsible for the increased PTK2 expression observed in HCC. Cheng et al. previously showed that Argonaute2 (Ago2), a protein involved in miRNA maturation, functions as a trans-activator by binding to the *PTK2* promoter [40]. Here, we found that PTK2 mRNA upregulation (118 cases) was more common than *PTK2* gene amplification (47 cases). Moreover, *PTK2* gene amplification was frequently detected concurrently with PTK2 mRNA upregulation (34 of 47 cases). Importantly, our results also indicated that *PTK2* promoter methylation regulated PTK2 expression in HCC patients, elucidating a new molecular mechanism underlying aberrant PTK2 expression and activation in HCC. However, further investigation is required to determine the precise mechanisms underlying the aberrant methylation of the *PTK2* promoter and *PTK2* amplification.

Conflicts of interest

The authors declare that they have no conflicts of interest.

Acknowledgements

This work was supported by the National Natural Science Foundation of China (81702936, 81822037, 81472589, 81672602, 81402345, 81502264 and 81872090), the Natural Science Foundation of Beijing (7172199), the Postdoctoral Science Foundation of China (2017M613389 and 2018T111142), and the Logistics Scientific Research project (BWS16J010), the Capital Foundation of Medical Developments (2016-4-5061).

Appendix A. Supplementary data

Supplementary data to this article can be found online at https://doi.org/10.1016/j.canlet.2019.02.040.

References

[1] A. Forner, J.M. Llovet, J. Bruix, Hepatocellular carcinoma, Lancet 379 (2012) 1245–1255.
[2] A. Jemal, F. Bray, M.M. Center, J. Ferlay, E. Ward, D. Forman, Global cancer statistics, Ca - Cancer J. Clin. 61 (2011) 69–90.
[3] H.B. El-Serag, Hepatocellular carcinoma, N. Engl. J. Med. 365 (2011) 1118–1127.
[4] B. Njei, Y. Rotman, I. Ditah, J.K. Lim, Emerging trends in hepatocellular carcinoma incidence and mortality, Hepatology 61 (2015) 191–199.
[5] J. Bruix, M. Sherman, D. American Association for, The Study of Liver, Management of hepatocellular carcinoma: an update, Hepatology 53 (2011) 1020–1022.
[6] T. Chiba, A. Iwama, O. Yokosuka, Cancer stem cells in hepatocellular carcinoma: therapeutic implications based on stem cell biology, Hepatol. Res. 46 (2016) 50–57.
[7] J.M. Llovet, S. Ricci, V. Mazzaferro, P. Hilgard, E. Gane, J.F. Blanc, A.C. de Oliveira, A. Santoro, J.L. Raoul, A. Forner, M. Schwartz, C. Porta, S. Zeuzem, L. Bolondi, T.F. Greten, P.R. Galle, J.F. Seitz, I. Borbath, D. Haussinger, T. Giannaris, M. Shan, M. Moscovici, D. Voliotis, J. Bruix, S.I.S. Group, Sorafenib in advanced hepatocellular carcinoma, N. Engl. J. Med. 359 (2008) 378–390.
[8] J. Chen, R. Jin, J. Zhao, J. Liu, H. Ying, H. Yan, S. Zhou, Y. Liang, D. Huang, X. Liang, H. Yu, H. Lin, X. Cai, Potential molecular, cellular and microenvironmental mechanism of sorafenib resistance in hepatocellular carcinoma, Cancer Lett. 367 (2015) 1–11.
[9] Y. Li, J. Laterra, Cancer stem cells: distinct entities or dynamically regulated phenotypes? Cancer Res. 72 (2012) 576–580.
[10] S.K. Mitra, D.D. Schlaepfer, Integrin-regulated FAK-Src signaling in normal and cancer cells, Curr. Opin. Cell Biol. 18 (2006) 516–523.
[11] S. Batista, E. Maniati, L.E. Reynolds, B. Tavora, D.M. Lees, I. Fernandez, G. Elia, O. Casanovas, C. Lo Celso, T. Hagemann, K. Hodivala-Dilke, Haematopoietic focal adhesion kinase deficiency alters haematopoietic homeostasis to drive tumour metastasis, Nat. Commun. 5 (2014) 5054.
[12] D.J. Sieg, C.R. Hauck, D. Ilic, C.K. Klingbeil, E. Schaefer, C.H. Damsky, D.D. Schlaepfer, FAK integrates growth-factor and integrin signals to promote cell migration, Nat. Cell Biol. 2 (2000) 249–256.
[13] X. Zhao, J.L. Guan, Focal adhesion kinase and its signaling pathways in cell migration and angiogenesis, Adv. Drug Deliv. Rev. 63 (2011) 610–615.
[14] S. Itoh, T. Maeda, M. Shimada, S. Aishima, K. Shirabe, S. Tanaka, Y. Maehara, Role of expression of focal adhesion kinase in progression of hepatocellular carcinoma, Clin. Cancer Res. 10 (2004) 2812–2817.
[15] G.W. McLean, N.O. Carragher, E. Avizienyte, J. Evans, V.G. Brunton, M.C. Frame, The role of focal-adhesion kinase in cancer - a new therapeutic opportunity, Nat. Rev. Canc. 5 (2005) 505–515.
[16] Y. Miyasaka, N. Enomoto, K. Nagayama, N. Izumi, F. Marumo, M. Watanabe, C. Sato, Analysis of differentially expressed genes in human hepatocellular carcinoma using suppression subtractive hybridization, Br. J. Canc. 85 (2001) 228–234.
[17] F.J. Sulzmaier, C. Jean, D.D. Schlaepfer, FAK in cancer: mechanistic findings and clinical applications, Nat. Rev. Canc. 14 (2014) 598–610.
[18] T. Fujii, K. Koshikawa, S. Nomoto, O. Okochi, T. Kaneko, S. Inoue, Y. Yatabe, S. Takeda, A. Nakao, Focal adhesion kinase is overexpressed in hepatocellular carcinoma and can be served as an independent prognostic factor, J. Hepatol. 41 (2004) 104–111.
[19] J.S. Chen, X.H. Huang, Q. Wang, X.L. Chen, X.H. Fu, H.X. Tan, L.J. Zhang, W. Li, J. Bi, FAK is involved in invasion and metastasis of hepatocellular carcinoma, Clin. Exp. Metastasis 27 (2010) 71–82.
[20] M. Luo, H. Fan, T. Nagy, H. Wei, C. Wang, S. Liu, M.S. Wicha, J.L. Guan, Mammary epithelial-specific ablation of the focal adhesion kinase suppresses mammary tumorigenesis by affecting mammary cancer stem/progenitor cells, Cancer Res. 69 (2009) 466–474.
[21] K.E. Williams, N.J. Bundred, G. Landberg, R.B. Clarke, G. Farnie, Focal adhesion kinase and Wnt signaling regulate human ductal carcinoma in situ stem cell activity and response to radiotherapy, Stem Cell. 33 (2015) 327–341.
[22] I.M. Shapiro, V.N. Kolev, C.M. Vidal, Y. Kadariya, J.E. Ring, Q. Wright, D.T. Weaver, C. Menges, M. Padval, A.I. McClatchey, Q. Xu, J.R. Testa, J.A. Pachter, Merlin deficiency predicts FAK inhibitor sensitivity: a synthetic lethal relationship, Sci. Transl. Med. 6 (2014) 237ra268.
[23] S.A. Park, M.J. Kim, S.Y. Park, J.S. Kim, W. Lim, J.S. Nam, Y. Yhong Sheen, TIMP-1 mediates TGF-beta-dependent crosstalk between hepatic stellate and cancer cells via FAK signaling, Sci. Rep. 5 (2015) 16492.
[24] L. Xu, X. Tong, S. Zhang, F. Yin, X. Li, H. Wei, C. Li, Y. Guo, J. Zhao, ASPP2 suppresses stem cell-like characteristics and chemoresistance by inhibiting the Src/FAK/Snail axis in hepatocellular carcinoma, Tumour Biol 37 (2016) 13669–13677.
[25] N. Panera, A. Crudele, I. Romito, D. Gnani, A. Alisi, Focal adhesion kinase: insight into molecular roles and functions in hepatocellular carcinoma, Int. J. Mol. Sci. 18 (2017).
[26] T. Yamada, M. Abei, I. Danjoh, R. Shirota, T. Yamashita, I. Hyodo, Y. Nakamura, Identification of a unique hepatocellular carcinoma line, Li-7, with CD13(+) cancer stem cells hierarchy and population change upon its differentiation during culture and effects of sorafenib, BMC Canc. 15 (2015) 260.
[27] J. Chen, M. Rajasekaran, K.M. Hui, Atypical regulators of Wnt/beta-catenin signaling as potential therapeutic targets in Hepatocellular Carcinoma, Exp. Biol. Med. 242 (2017) 1142–1149.
[28] T. Shimizu, K. Fukuoka, M. Takeda, T. Iwasa, T. Yoshida, J. Horobin, M. Keegan, L. Vaickus, A. Chavan, M. Padval, K. Nakagawa, A first-in-Asian phase 1 study to evaluate safety, pharmacokinetics and clinical activity of VS-6063, a focal adhesion kinase (FAK) inhibitor in Japanese patients with advanced solid tumors, Cancer Chemother. Pharmacol. 77 (2016) 997–1003.
[29] S.F. Jones, L.L. Siu, J.C. Bendell, J.M. Cleary, A.R. Razak, J.R. Infante, S.S. Pandya, P.L. Bedard, K.J. Pierce, B. Houk, W.G. Roberts, S.M. Shreeve, G.I. Shapiro, A phase I study of VS-6063, a second-generation focal adhesion kinase inhibitor, in patients with advanced solid tumors, Investig. New Drugs 33 (2015) 1100–1107.
[30] J.C. Soria, H.K. Gan, S.P. Blagden, R. Plummer, H.T. Arkenau, M. Ranson, T.R. Evans, G. Zalcman, R. Bahleda, A. Hollebecque, C. Lemech, E. Dean, J. Brown, D. Gibson, V. Peddareddigari, S. Murray, N. Nebot, J. Mazumdar, L. Swartz, K.R. Auger, R.A. Fleming, R. Singh, M. Millward, A phase I, pharmacokinetic and pharmacodynamic study of GSK2256098, a focal adhesion kinase inhibitor, in patients with advanced solid tumors, Ann. Oncol. 27 (2016) 2268–2274.
[31] M. Dean, T. Fojo, S. Bates, Tumour stem cells and drug resistance, Nat. Rev. Canc. 5 (2005) 275–284.
[32] T. Yamashita, X.W. Wang, Cancer stem cells in the development of liver cancer, J. Clin. Investig. 123 (2013) 1911–1918.
[33] K. Taniguchi, L.R. Roberts, I.N. Aderca, X. Dong, C. Qian, L.M. Murphy, D.M. Nagorney, L.J. Burgart, P.C. Roche, D.I. Smith, J.A. Ross, W. Liu, Mutational spectrum of beta-catenin, AXIN1, and AXIN2 in hepatocellular carcinomas and hepatoblastomas, Oncogene 21 (2002) 4863–4871.
[34] C.M. Wong, S.T. Fan, I.O. Ng, beta-Catenin mutation and overexpression in hepatocellular carcinoma: clinicopathologic and prognostic significance, Cancer 92 (2001) 136–145.
[35] C. Gao, G. Chen, S.F. Kuan, D.H. Zhang, D.D. Schlaepfer, J. Hu, FAK/PYK2 promotes the Wnt/beta-catenin pathway and intestinal tumorigenesis by phosphorylating GSK3beta, Elife 4 (2015).
[36] S.M. Ahn, S.J. Jang, J.H. Shim, D. Kim, S.M. Hong, C.O. Sung, D. Baek, F. Haq, A.A. Ansari, S.Y. Lee, S.M. Chun, S. Choi, H.J. Choi, J. Kim, S. Kim, S. Hwang, Y.J. Lee, J.E. Lee, W.R. Jung, H.Y. Jang, E. Yang, W.K. Sung, N.P. Lee, M. Mao, C. Lee, J. Zucman-Rossi, E. Yu, H.C. Lee, G. Kong, Genomic portrait of resectable hepatocellular carcinomas: implications of RB1 and FGF19 aberrations for patient stratification, Hepatology 60 (2014) 1972–1982.
[37] J. Gao, B.A. Aksoy, U. Dogrusoz, G. Dresdner, B. Gross, S.O. Sumer, Y. Sun, A. Jacobsen, R. Sinha, E. Larsson, E. Cerami, C. Sander, N. Schultz, Integrative analysis of complex cancer genomics and clinical profiles using the cBioPortal, Sci. Signal. 6 (2013) pl1.
[38] Z. Kan, H. Zheng, X. Liu, S. Li, T.D. Barber, Z. Gong, H. Gao, K. Hao, M.D. Willard, J. Xu, R. Hauptschein, P.A. Rejto, J. Fernandez, G. Wang, Q. Zhang, B. Wang, R. Chen, J. Wang, N.P. Lee, W. Zhou, Z. Lin, Z. Peng, K. Yi, S. Chen, L. Li, X. Fan, J. Yang, R. Ye, J. Ju, K. Wang, H. Estrella, S. Deng, P. Wei, M. Qiu, I.H. Wulur, J. Liu, M.E. Ehsani, C. Zhang, A. Loboda, W.K. Sung, A. Aggarwal, R.T. Poon, S.T. Fan, J. Wang, J. Hardwick, C. Reinhard, H. Dai, Y. Li, J.M. Luk, M. Mao, Whole-genome sequencing identifies recurrent mutations in hepatocellular carcinoma, Genome Res. 23 (2013) 1422–1433.
[39] H. Okamoto, K. Yasui, C. Zhao, S. Arii, J. Inazawa, PTK2 and EIF3S3 genes may be amplification targets at 8q23-q24 and are associated with large hepatocellular carcinomas, Hepatology 38 (2003) 1242–1249.
[40] N. Cheng, Y. Li, Z.G. Han, Argonaute2 promotes tumor metastasis by way of up-regulating focal adhesion kinase expression in hepatocellular carcinoma, Hepatology 57 (2013) 1906–1918.